DEVELOPMENT OF VANADIUM-PHOSPHATE CATALYSTS FOR METHANOL PRODUCTION BY SELECTIVE OXIDATION OF METHANE

QUARTERLY TECHNICAL PROGRESS REPORT 17

April 1 - June 31, 1997

By
Robert L. McCormick (Principal Investigator)
Gokhan O. Alptekin (Graduate Assistant)

July 30, 1997

DOE Contract No. DE-AC22-92PC92110

Department of Chemical Engineering and Petroleum Refining
and
Colorado Institute for Fuels and High-Altitude Engine Research

Colorado School of Mines
Golden, Colorado 80403-1887

FINAL

DISCLAIMER

TABLE OF CONTENTS

LIST OF FIGURES

LIST OF TABLES

EXECUTIVE SUMMARY

This document is the seventeenth quarterly technical progress report under Contract No. DE-AC22-92PC92110 "Development of Vanadium-Phosphate Catalysts for Methanol Production by Selective Oxidation of Methane" and covers the period April-June, 1997. Vanadium phosphate, vanadyl pyrophosphate specifically, is used commercially to oxidize butane to maleic anhydride and is one of the few examples of an active and selective oxidation catalyst for alkanes. In this project we are examining this catalyst for the methane oxidation reaction. Initial process variable and kinetic studies indicated that vanadyl pyrophosphate is a reasonably active catalyst below 500°C but produces CO as the primary product, no formaldehyde or methanol were observed.

A number of approaches for modification of the catalyst to improve selectivity have been tried. Results obtained earlier in this project are summarized under Project Description in the body of this report. Iron phosphate and iron phosphate supported on silica catalysts have been shown in our previous work to produce much higher yields of partial oxidation products from methane than VPO. During this quarter we have expanded these studies dramatically by detailed testing of a new silica support, by performance of detailed kinetic and product selectivity studies on the quartz form of $FePO_4$, both unsupported and supported on silica, by testing of a mixed valence iron phosphate $Fe_4(P_2O_7)$, and by detailed characterization of these and other materials by a number of methods including Mossbauer spectroscopy.

The most selective catalyst examined to date is $FePO_4$ supported on silica. This material has produced formaldehyde with space time yields of nearly 500 g/kg-h. Methanol yields are low but quantifiable at roughly 10 g/kg-h. Interestingly, addition of water to the feed gas produces large improvements in the formaldehyde yield by suppression of the parallel reaction to form carbon dioxide. Increasing oxygen partial pressure over this catalyst did not produce the expected drop in formaldehyde yield and in fact, formaldehyde yield actually increased.

Characterization via Mossbauer spectroscopy appears to be a very valuable tool for examination of the iron phosphate system. Spectra of several fresh catalysts were obtained providing detailed information on the chemical environment of iron. While detailed analyses of these data have not yet been completed, it is apparent that iron exists in different chemical states in all of the catalytic materials being studied. Interestingly, the Fe-promoted VPO catalyst is shown to contain a small fraction of Fe^{2+} by Mossbauer. This results is unexpected an may have important implications for the mechanism of the promoting effect as well as for the role of mixed valence species in iron phosphate methane oxidation catalysts.

Additionally, in May a poster describing the results for VPO was presented at the North American Catalysis Society Meeting in Chicago. A paper describing these results has also been accepted for publication in Journal of Catalysis.

1. INTRODUCTION

This document is the seventeenth quarterly technical progress report under Contract No. DE-AC22-92PC92110 "Development of Vanadium-Phosphate Catalysts for Methanol Production by Selective Oxidation of Methane" and covers the period April-June, 1997. The basic premise of this project is that vanadyl pyrophosphate (VPO), a catalyst used commercially in the selective oxidation of butane to maleic anhydride, can be developed as a catalyst for selective methane oxidation. Data supporting this idea include published reports indicating moderate to high selectivity in oxidation of ethane (Michalakos, et al., 1993), propane (Ai, 1986), and pentane (Busca and Centi, 1989), as well as butane (Centi, et al., 1988). Methane oxidation is a much more difficult reaction to catalyze than that of other alkanes and it is expected that considerable modification of vanadyl pyrophosphate will be required for this application. It is well known that VPO can be modified extensively with a large number of different promoters and in particular that promoters can enhance selectivity and lower the temperature required for butane conversion (Hutchings, 1991).

Preliminary results have shown that CO is the primary product of methane oxidation over this catalyst at temperatures below 500°C. Several approaches have been or are being taken to improve catalyst selectivity. These include:

- Modification of the surface acidity of vanadyl pyrophosphate through production of structural defects and exchange of surface hydroxyl groups.
- Promotion of the catalyst by addition of first row transition metals, especially Fe.
- Attempts to prepare vanadyl pyrophosphate on a silica support.
- Examination of iron phosphate and silica supported iron phosphates for the methane oxidation reaction.

Modification of acidity was not successful at improving methane oxidation selectivity. Attempts at supporting vanadyl pyrophosphate have also not been successful. Promotion with Cr and Fe produced significant yields of formaldehyde. Iron phosphate ($FePO_4$) and silica supported iron phosphate have much higher formaldehyde selectivities (up to 500 g/kg-h) and methanol was observed as a quantifiable product. Addition of water to the feed results in a large enhancement in yield. Iron phosphates have been the focus of our work this quarter.

2. PROJECT DESCRIPTION

2.1. Objectives

The original objectives of this project are:

- To determine optimum conditions for methanol and formaldehyde production from methane using VPO catalysts.
- To utilize promoters and catalyst supports to improve oxygenate yield relative to the base case catalysts.
- To provide a preliminary understanding of how these promoters and supports actually effect catalyst properties.
- Use the information obtained to prepare advanced catalysts which will be tested for activity, selectivity, and stability.

2.2. Project Overview

The goal of the project is to develop a catalyst which allows methane oxidation to methanol to be conducted at high conversion and selectivity. The catalyst development strategy is to utilize promoters and supports to improve the activity and selectivity of the unmodified VPO catalyst.

The project is divided into four tasks:

Task 1: Laboratory Setup. Work on this task has been completed.

Task 2: Process and Catalyst Variable Study. Vanadyl pyrophosphate has not been found to be a selective catalyst for methane oxidation. Results have been summarized in previous reports

Task 3: The Effect of Promoters and Supports. To date we have tested catalysts promoted with the first row transition metals and observed increased selectivity to HCHO for Fe and Cr. Attempts at putting vanadyl pyrophosphate on a support are underway.

Task 4: Advanced Catalyst Testing. Our first advanced catalysts are iron phosphates, based on a recent literature report (Wang and Otsuka, 1995) and our own observation of the promoting effect of Fe.

Thus, Tasks 3 and 4 are on going. From a technical standpoint the catalyst development approaches we have followed are outlined below.

2.2.1. Modification of Surface Acidity. It has been shown that strong Lewis acid sites on the surface of VPO are responsible for initial alkane activation (Busca, et al., 1986a). This Lewis acidity is thought to be caused by lattice defects or strain initiated by disorder in stacking of the layers of VPO (Busca, et al, 1986b; Horowitz, et al, 1988). One approach we have taken is directed at increasing the strength of these strong Lewis acid

sites by enhanced strain or disorder in the layer stacking. By increasing Lewis acid site strength it is hoped that the temperature required for methane activation can be lowered resulting in improved selectivity. Bronsted acid sites have also been removed by exchange of protons with potassium under nearly anhydrous conditions. The degree of disorder of these materials was measured by XRD line broadening. Surface acidity of these materials was measured by FTIR of chemisorbed bases and by activity in methanol coupling to dimethyl ether. Activity and selectivity in methane oxidation were also measured. XRD indicates that modifications were successful at introducing disorder in the layer stacking. The methanol conversion results suggest that these catalysts do have more acid sites. IR suggests that sites on one of the catalysts may be of higher strength but the results are not conclusive. The potassium exchanged catalyst was poorly active in the methanol conversion reaction. The catalysts with enhanced acidity as gauged by methanol conversion were more active for methane conversion but not more selective than unmodified vanadyl pyrophosphate. While not a high priority, we may measure the number of acid sites in these materials by ammonia chemisorption in a TGA apparatus to confirm our ideas.

2.2.2. Supported Vanadyl Pyrophosphate. Because of the complex procedure required to prepare $(VO)_2P_2O_7$, it is very difficult to place on a support and no examples are available in the academic or patent literature. We have tried several approaches but none has yielded the desired phase on the support. This avenue of investigation may not be pursued further unless we come up with a new idea that has a high probability of success.

2.2.3. Promotion by First Row Transition Metals. Vanadyl pyrophosphate samples promoted with Mn, Cr, Fe, Co, Cu, and Zn have been prepared by addition of promoter salts to a suspension of the activated catalyst. Promotion with Fe and Cr have produced significant changes in catalyst activity and selectivity with measurable yields of formaldehyde at low conversions. Surface and bulk analysis of these materials indicates incorporation of the promoter on both the surface and bulk at a promoter:V ratio of roughly 1:10. Catalyst characterization indicates that promoters stabilize some of the vanadium in the 5+ oxidation state and we hypothesize that this is responsible for the improved selectivity.

2.2.4. Iron Phosphate Based Catalysts. Crystalline $FePO_4$ was tested in methane oxidation because of the interesting results noted for Fe promotion of vanadium phosphate and because of literature reports suggesting that it was an active and selective catalyst. Preliminary experiments reported previously indicated 30% selectivity to formaldehyde at 1% conversion, a much higher yield that observed of the vanadium phosphates. This result will be expanded upon and confirmed in the coming months. $FePO_4$ is also easily prepared on a silica support. This material exhibited a formaldehyde selectivity near 40% at 1% conversion. The activation energy for methane oxidation was much higher over this material than over vanadium phosphate or unsupported iron phosphate and was similar to values observed for methane oxidation over silica itself. X-ray diffraction data indicate the presence of the quartz polymorph of $FePO_4$ in both unsupported and supported catalysts. The iron phosphate system appears to be much

more interesting for the methane oxidation reaction than vanadium phosphate. There are several stable crystalline phases of iron phosphate and a great deal of practical research remains to be done on this system. Our focus for the remainder of the project is expected to be iron phosphates.

3. PROJECT STATUS

3.1. Steady-state Reactor Studies

3.1.1. SiO_2 Support

Previously, silicon oxide was used to support the crystalline iron phosphate quartz phase (referred as $FePO_4$(Q) in this report) and significant space time yields of formaldehyde was observed over the silica supported $FePO_4$(Q). In these experiments, silica support itself was found to be very active and selective, rather than being inert for methane oxidation. It was particularly important to measure the activity of the support to determine the best material for this application. Silicon oxide catalysts prepared by different methods were tested and significantly different catalytic activity and selectivity patterns were observed for these different preparations (also discussed in the literature by Parmaliana, et al., 1991). Among these preparations, fumed silica (99.8%, Aldrich) was found to be the least active, while the silica prepared by precipitation was the most active one. Two different silica supports prepared by precipitation SiO_2-OR (99.6%, BDH Chemicals) and SiO_2-AW (99.8%, Cerac Chemicals) were investigated in detail. These silica supports were washed with a nonpolar acid to reduce the Na content.

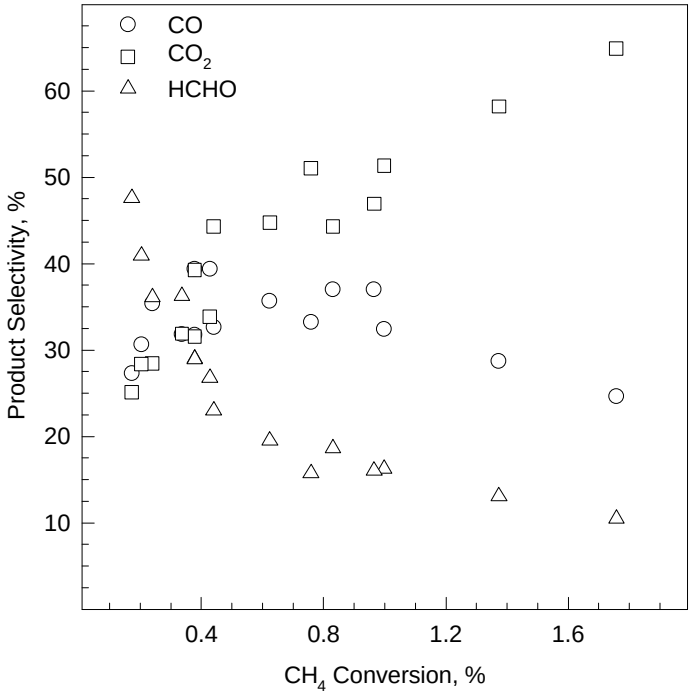

Figure 1. Product selectivity as a function of CH_4 conversion over SiO_2-AW catalyst. *P_{CH4} = 37.6 kPa, P_{O2} = 3.1 kPa, CH_4:O_2 = 12 ,GHSV = 10,000 - 30,000 hr^{-1}, T= 848-898 K.*

In the literature, it was speculated that even traces of Na may cause significant deactivation of the catalyst. The not-acid-washed silicon oxide catalyst, SiO_2-NAW (99.8% Cerac Chemicals), was also tested for methane oxidation to clarify the effect of acid washing.

Product selectivity as a function of methane conversion over the SiO_2-AW catalyst is presented by Figure 1. In these experiments, conversion was varied by varying the space time. Experiments were repeated in the temperature range of 848 to 898 K. HCHO selectivity was observed to be high at low methane conversion levels and decreases to 20% at 1% conversion. CO_2 was the principal product above 1% conversion. CO selectivity increases as formaldehyde selectivity goes down, which may indicate an oxidation path from formaldehyde to CO. High CO_2 selectivity even at very low conversion levels may suggest a direct oxidation route from CH_4 to CO_2,which is also observed for V_2O_5/SiO_2 systems (Spencer, et al., 1989).

Selectivity-conversion pattern observed for the SiO_2-OR presented in Figure 2 was found to be very similar to that of SiO_2-AW catalyst. Even the surface area of the SiO_2-OR catalyst is much lower, it is a more active catalyst than SiO_2-AW for CH_4 oxidation. Formaldehyde selectivity at 1% conversion was about 10% over the SiO_2-OR, which is slightly lower than the one observed for SiO_2-AW.

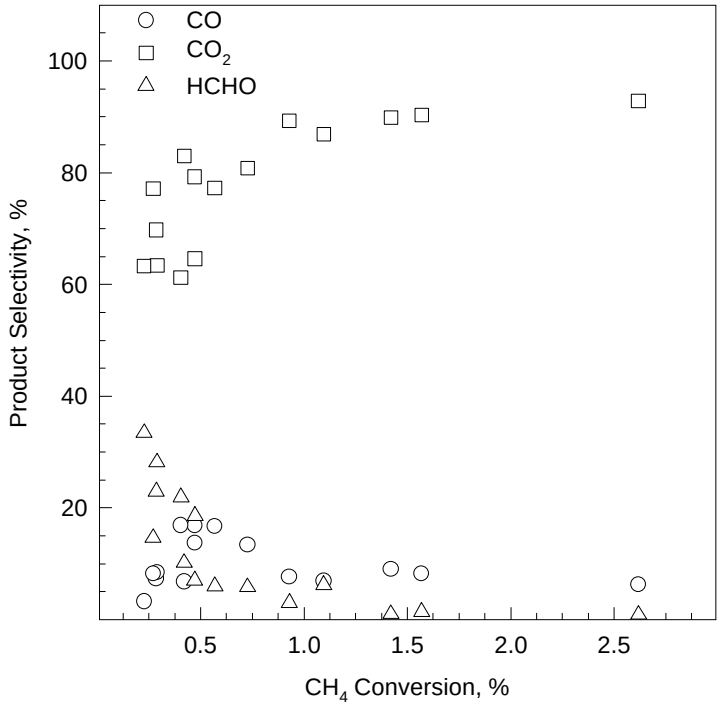

Figure 2. Product selectivity as a function of CH_4 conversion over SiO_2-OR catalyst. *P_{CH4} = 37.6 kPa, P_{O2} = 3.1 kPa, CH_4:O_2 = 12 , GHSV = 10,000 - 30,000 hr^{-1}, T= 848-898 K.*

A power law rate model was applied to describe the kinetics of methane oxidation over SiO_2-AW and SiO_2-OR catalysts.

$$-r_{CH4} = k\, P_{CH4}^{\alpha}\, P_{O2}^{\beta}$$

To determine the reaction orders in oxygen and methane (α and β), partial pressures of these species were kept constant one at a time while varying the other, and the reaction rate was measured. Gas hourly space velocity (GHSV) was also kept constant in these experiments. Effect of methane and oxygen partial pressures on the reaction rate is given in Figure 3 and 4.

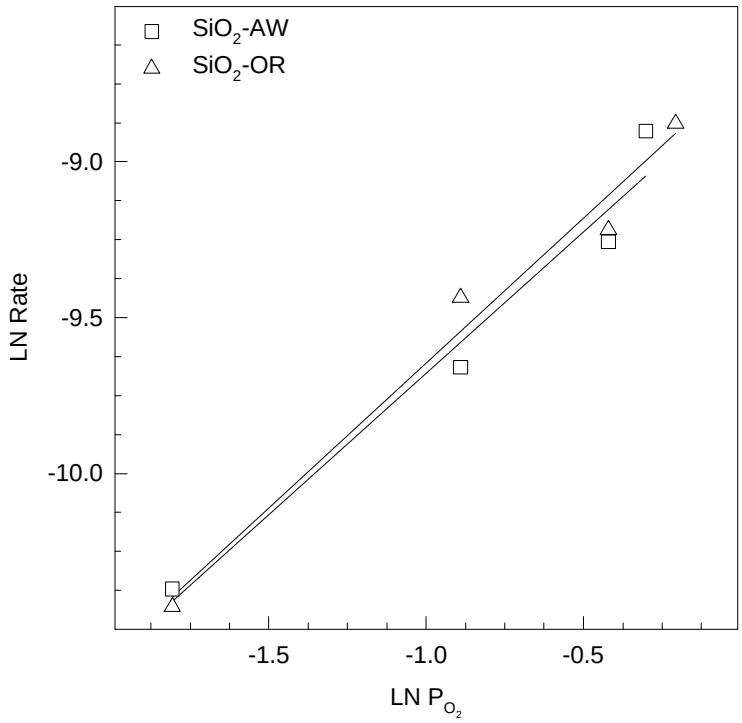

Figure 3. Effect of CH_4 partial pressure on CH_4 oxidation rate over SiO_2-AW and SiO_2-OR catalysts. *P_{CH4} = 16.7-82.2 kPa, P_{O2} = 3.1 kPa,GHSV = 12,750 hr^{-1}, T=873 K.*

The reaction orders for methane and oxygen were calculated as 0.91 and 0.32, and 0.93 and 0.31 for SiO_2-AW and SiO_2-OR catalysts, respectively. A first order reaction in CH_4 partial pressure agrees with the reported literature (Parmaliana, et al., 1991), but a fractional reaction order of 0.3 in O_2 partial pressure is quite unusual for CH_4 oxidation catalysts. Previously, over the vanadium phosphate systems we have reported very little or no dependence on the oxygen concentration, but oxygen concentration effects the methane oxidation rate positively in the case of silicon oxide catalysts.

Activation energy of methane oxidation over the SiO_2-AW and SiO_2-OR was also calculated as 184 and 142 kJ/mole, respectively. An Arrhenius plot is given in Figure 4 for these catalysts. This activation energy value is very typical to the ones reported in the literature for different silica preparations (Kastanas, et al., 1988). The linear nature of

this plot even at the highest conversion levels insures the absence of mass and heat transfer effects. Pore diffusion limitation is particularly important to avoid, since the SiO_2-AW is an extremely high surface area catalyst (~600 m^2/g).

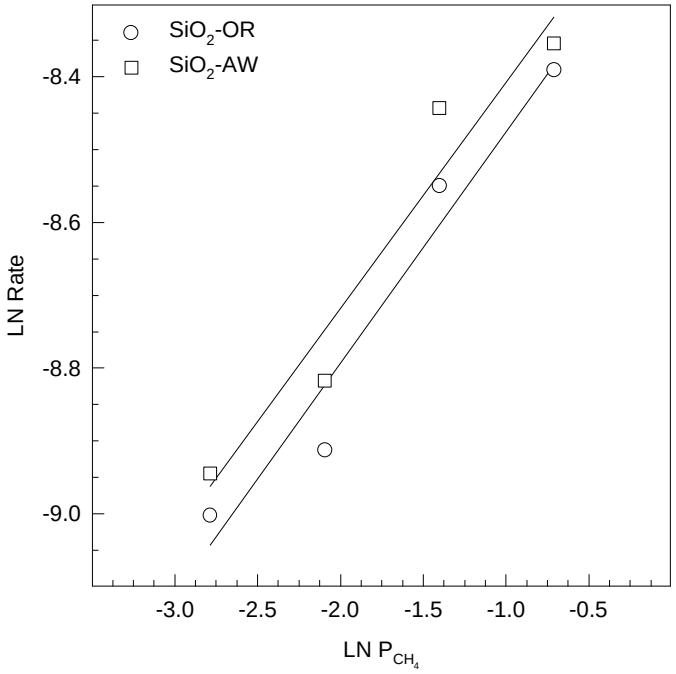

Figure 4. Effect of O_2 partial pressure on CH_4 oxidation rate over SiO_2-AW and SiO_2-OR catalysts. *P_{CH4}= 49.8 kPa, P_{O2} =6.2-49.8 kPa, GHSV = 12,750 hr^{-1}, T = 873 K.*

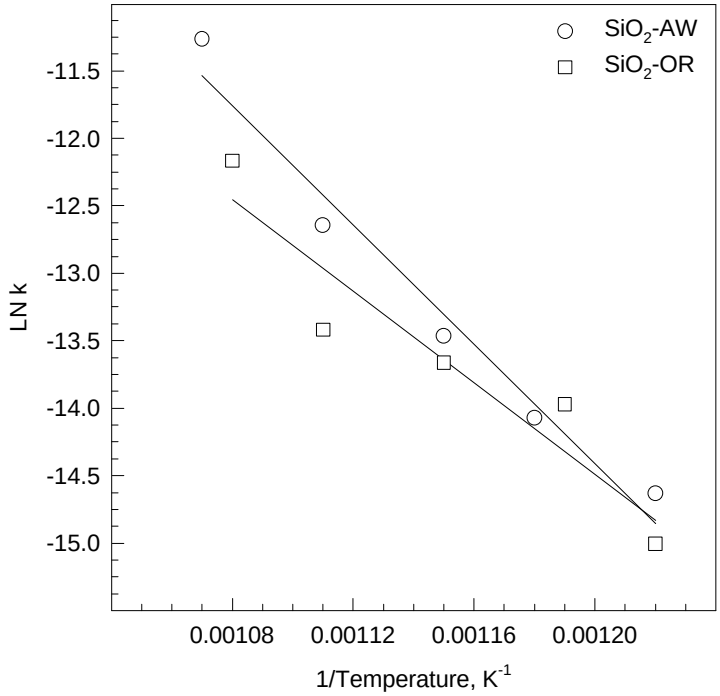

Figure 5. Arrhenius plot for CH_4 oxidation over SiO_2-AW and SiO_2-OR catalysts. *P_{CH4} = 50.1 kPa, P_{O2} = 3.1 kPa, CH_4:O_2 = 12, GHSV = 21,000 hr^{-1}, T= 823-933 K.*

Formaldehyde space time yields (STY) in the range of 7-113 g/kg h were observed over the SiO_2-AW. Interestingly, higher formaldehyde yields were observed at high oxygen partial pressures. Formaldehyde selectivity, on the other hand, was favored at low oxygen concentrations (i.e. high CH_4:O_2 ratio).

For the SiO_2-OR catalyst space time yield of formaldehyde was slightly lower than the SiO_2-AW (in the range of 5 to 92 g/kg h). For the new supported iron phosphate catalyst preparations SiO_2-AW will be used as the support material.

The effect of acid washing on the catalytic activity was also tested for SiO_2 catalysts. The not-acid-washed silicon oxide, SiO_2-NAW catalyst, was found to be less active than nitric acid washed SiO_2-AW. Formaldehyde selectivity and space time yield were also lower for the SiO_2-NAW. Figure 6a and 6b presents a comparison of the methane conversion and formaldehyde space time yield for the acid washed and not-acid-washed precipitated silicon oxide catalysts.

3.1.2. $FePO_4$ Quartz Phase

Given the very interesting results reported for methane oxidation over these catalysts previously, the focus of our work on advanced catalysts was on the studies on iron phosphate materials. Note that a report in the literature has appeared on methane conversion over iron phosphate (Wang and Otsuka, 1995).

Depending on the preparation and activation conditions and on the P:Fe ratio, $FePO_4$ can be prepared in two different structures. The first one is the well known quartz like phase structure with a P:Fe ratio of 1.0. This structure is comparable to that of SiO_2 due to the alternated substitution of one FeO_4 tetrahedron and one PO_4 tetrahedron for two SiO_4 tetrahedra. A tridymite type phase is also observed in the presence of an excess of phosphorous, and it can be stabilized at lower temperatures (733-803 K).

In this quarter, the quartz phase of $FePO_4$ was investigated in detail for CH_4 oxidation. Formaldehyde was the only selective product observed in these experiments. The conversion-selectivity plot presented in Figure 7 indicates that HCHO selectivity is higher at lower CH_4 conversion levels. CO selectivity approaches zero at very low conversions which suggests that it is a secondary product.

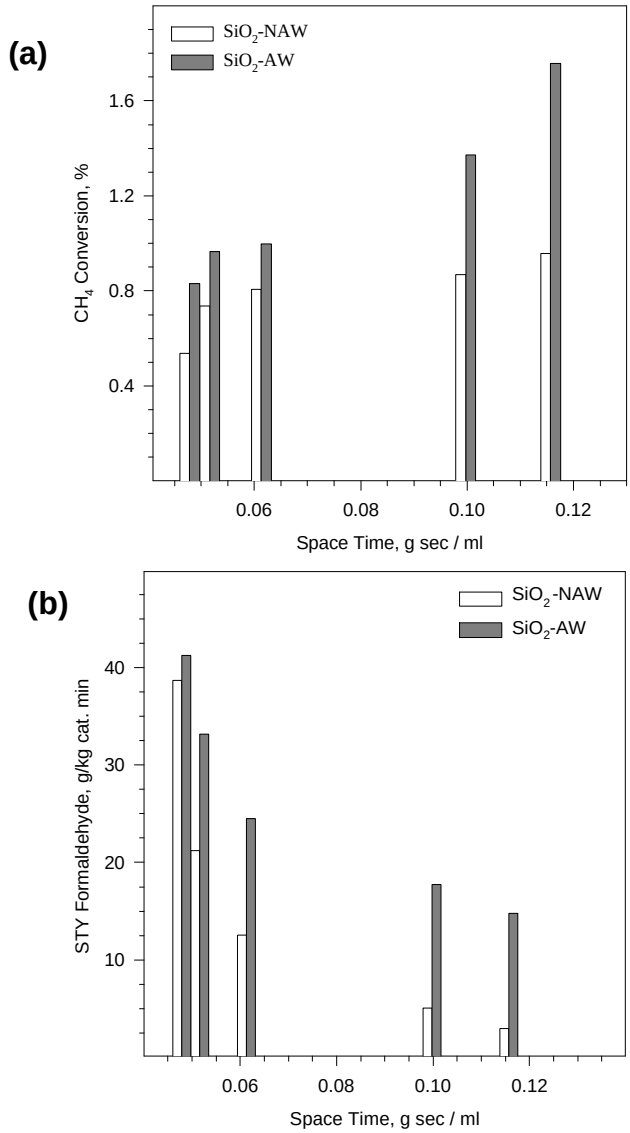

Figure 6. A comparison of **(a)** CH_4 conversion, **(b)** Formaldehyde STY for regular and acid washed SiO_2 catalysts. *P_{CH4}= 16.7-82.2 kPa, P_{O2}= 3.1 kPa, GHSV= 12,750 hr^{-1}, T=873 K.*

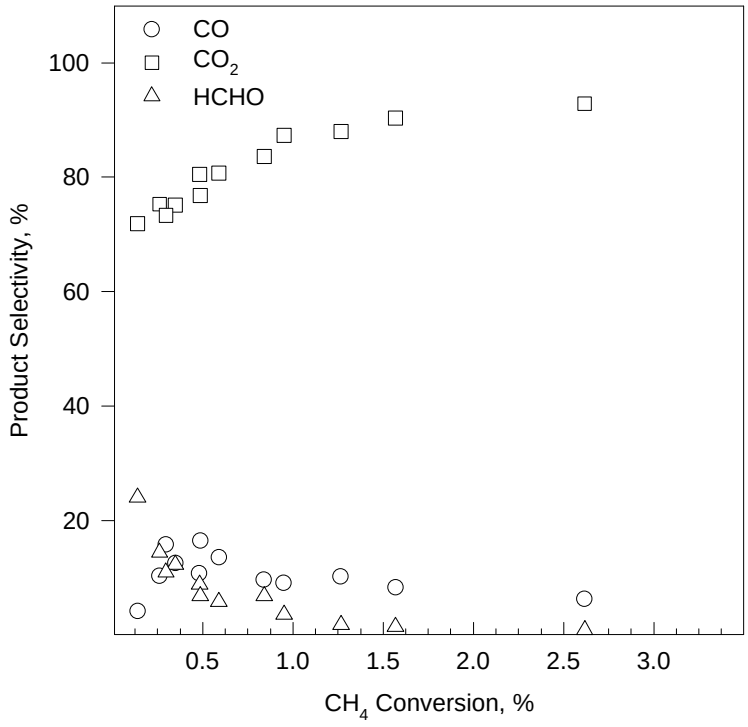

Figure 7. Product selectivity as a function of CH_4 conversion over $FePO_4$(Q) catalyst. *P_{CH4} = 37.6 kPa, P_{O2} = 3.1 kPa, CH_4:O_2 = 12 ,GHSV = 10,000 - 30,000 hr^{-1}, T= 848-898 K.*

Interestingly, even at low conversion conditions, CO_2 selectivity is high. This may be explained with the presence of a direct oxidation path from CH_4 to CO_2.

It is well known that in the presence of steam the iron phosphates can form mixed valence hydroxyphosphates that are active and selective catalysts for other oxidation reactions (Millet and Vedrine, 1995), so the use of steam was attempted. As the selectivity-conversion plot presented by Figure 8 indicates, the presence of steam in the feed stream causes a decrease in the CO_2 selectivity. CO and HCHO selectivity, as well as space time yield of formaldehyde increases when steam is co-fed. During these experiments, steam partial pressure was varied in 3.1 to 9.3 kPa range, keeping the GHSV constant. The effect of CH_4, O_2 and H_2O partial pressures on space time yield of formaldehyde are presented by Figure 9a and 9b.

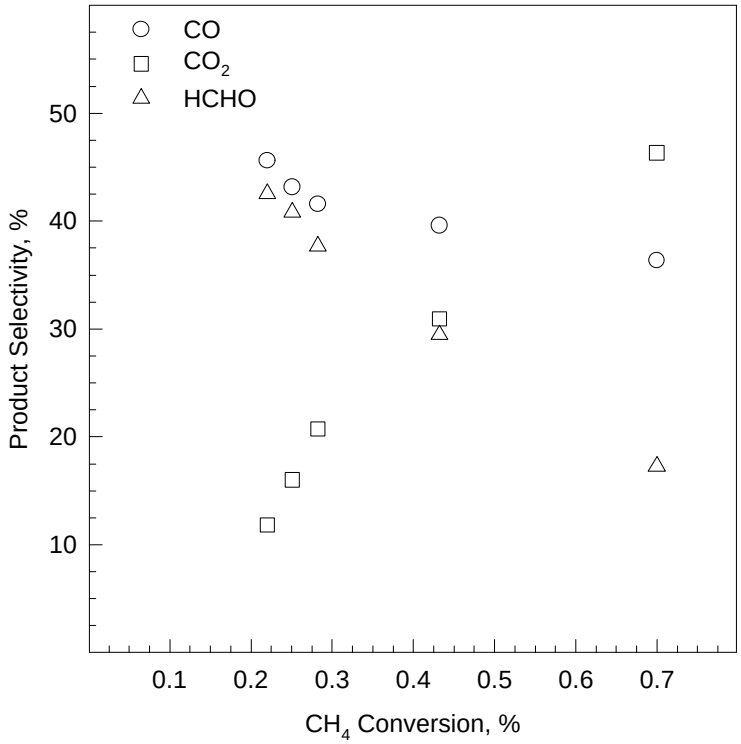

Figure 8. Product selectivity as a function of CH_4 conversion over $FePO_4$(Q) in the presence of water in the feed stream. *P_{CH4} = 37.6 kPa, P_{O2} = 3.1 kPa, P_{H2O} = 3.1 kPa, CH_4:O_2 = 12 , GHSV = 10,000 - 30,000 hr^{-1}, T= 848-898 K.*

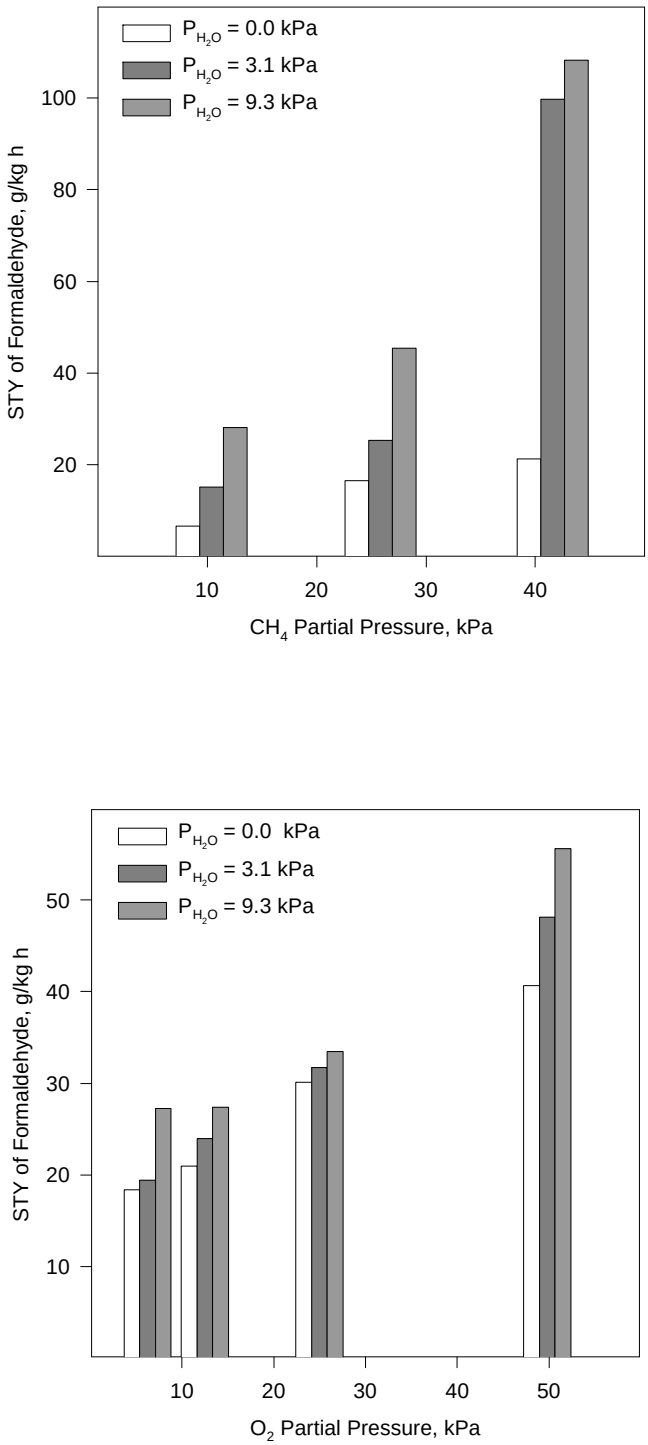

Figure 9. Effect of **(a)** CH_4 and **(b)** O_2 partial pressure on STY of HCHO in the absence and presence of water.

Feeding steam with the reacting mixture has significant effects on formaldehyde yield and selectivity. Highest formaldehyde space time yield observed for the $FePO_4(Q)$ in the absence and in the presence of steam were 59 and 148 g/kg h, respectively. In these experiments no methanol had been formed. High O_2 partial pressure as well as CH_4 partial pressure promoted the formaldehyde yield.

Effect of CH_4 and O_2 partial pressures were examined in order to determine to optimum operating conditions to maximize formaldehyde yields. The slope of the lines in Figure 10 and 11 represents the reaction orders of CH_4 and O_2 for a power law rate model. In the next quarter, a more detailed rate model will be developed involving the steam partial pressure.

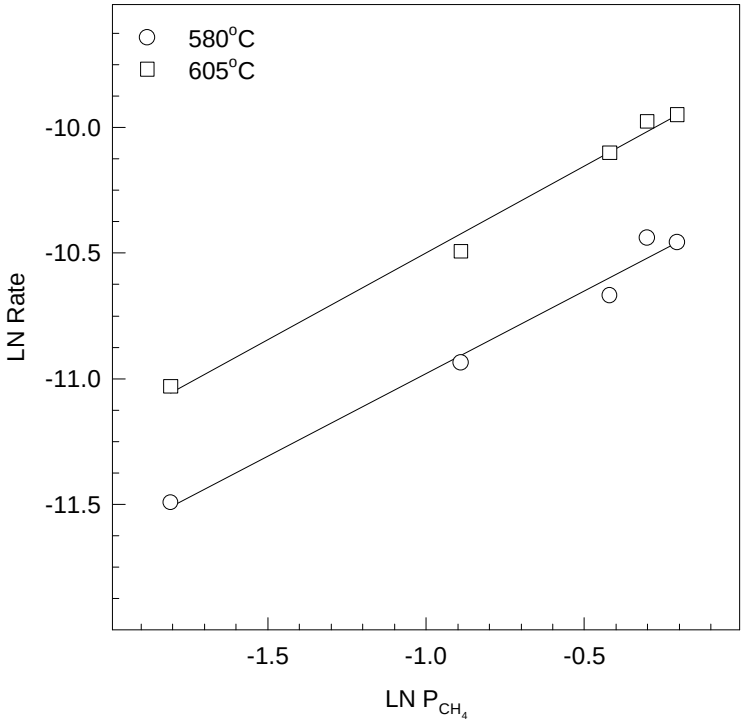

Figure 10. Effect of CH_4 partial pressure on CH_4 oxidation rate over $FePO_4(Q)$ catalyst. *P_{CH4} = 16.7-82.2 kPa, P_{O2} = 3.1 kPa, GHSV = 12,750 hr^{-1}.*

Reaction orders for CH_4 and O_2 were calculated as 0.66 and 0.45, respectively. These experiments were repeated at different temperatures, and the influence of temperature on the reaction orders was found to be negligible in the range studied.

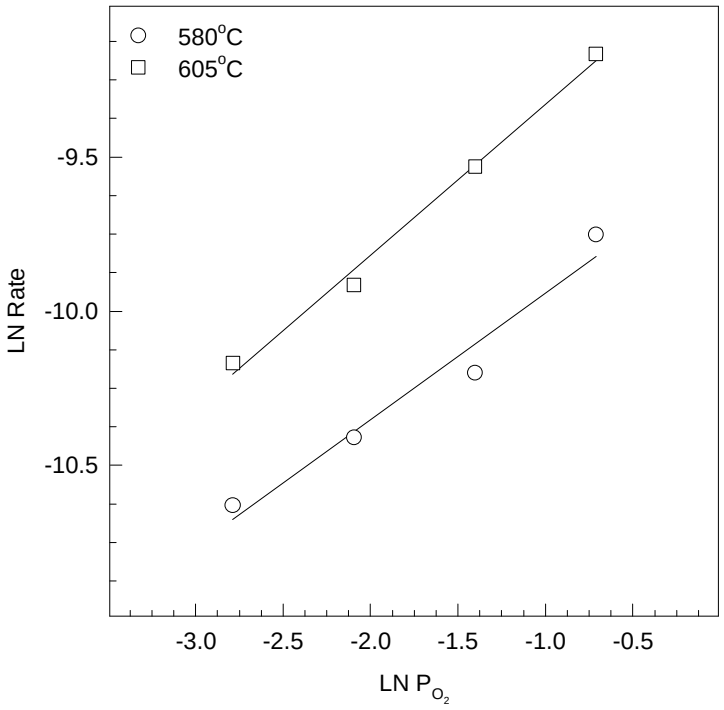

Figure 11. Effect of O_2 partial pressure on CH_4 oxidation rate over $FePO_4$(Q) catalyst. *P_{CH4} = 49.8 kPa, P_{O2} =6.2-49.8 kPa, GHSV = 12,750 hr^{-1}.*

3.1.3. $FePO_4/SiO_2$ (5%)

This catalyst was prepared by impregnation of $FePO_4$ quartz phase over the SiO_2-OR support. In our preliminary experiments, over $FePO_4$(Q)/SiO_2 (5% wt.) poorly quantifiable methanol traces were evident in the reactor effluent. Gas Chromatography (GC) method was improved to obtain better quantification for methanol peaks. This was mainly done by using a longer Poropak-T column which eliminated the interference of the tail of water peak with the methanol peak.

In this quarter, $FePO_4$(Q)/SiO_2 (5%) catalyst was investigated in detail, with the new GC method. Supporting $FePO_4$(Q) with silicon oxide caused an appreciable synergetic effect on the catalytic activity and selectivity. Quantifiable amounts of methanol and high formaldehyde space time yields were observed. A selectivity-conversion plot for this catalyst is presented in Figure 12 . These results indicates that a 40% formaldehyde selectivity can be achieved over 1-2% conversion level. CO_2 selectivity was observed to be low at low methane conversion levels unlike the ones we observed for SiO_2-OR and $FePO_4$(Q).

Methane formation into methanol was more favorable if the CH_4:O_2 ratio was kept high (i.e. 22.5 and above). On the other hand, higher space time yield of formaldehyde can be achieved at higher oxygen partial pressure levels.

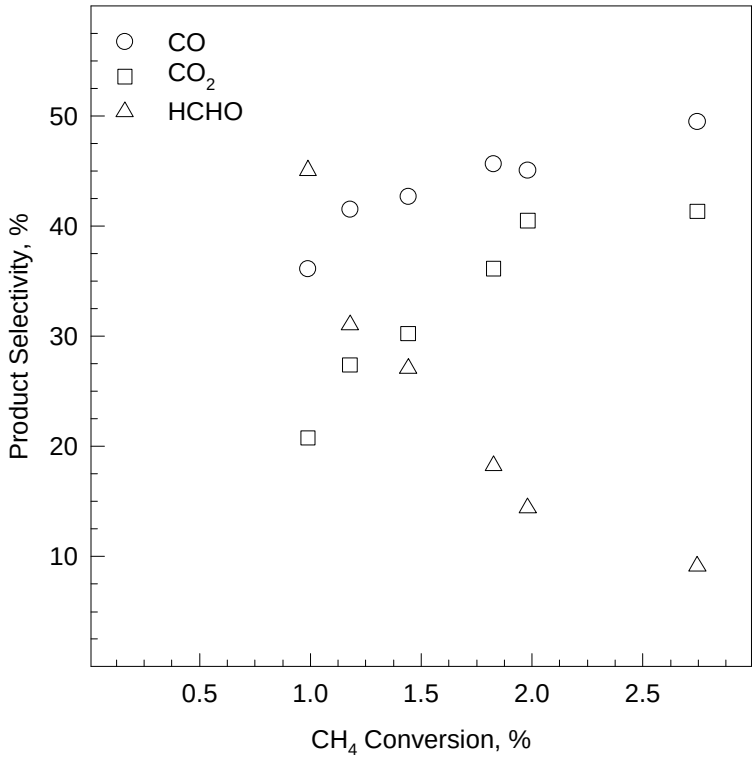

Figure 12. Product selectivity as a function of CH_4 conversion over $FePO_4(Q)/SiO_2$ catalyst. *P_{CH4} = 37.6 kPa, P_{O2} = 3.1 kPa, CH_4:O_2 = 12 , GHSV = 10,000 - 30,000 hr^{-1}, T= 898 K.*

Space time yields of HCHO and CH_3OH as a function of CH_4:O_2 ratio are given in Figure 13. Higher STY of formaldehyde was observed at higher temperatures, but CH_3OH formation is favorable at relatively low temperatures (i.e. 858 K).

A simple power law model was applied to describe the kinetics of methane oxidation. The reaction orders in CH_4 and O_2 were determined as described earlier in this report.

To determine the effect of methane partial pressure on methane oxidation rate methane partial pressure was changed in the range of 16.7 to 82.2 kPa, keeping the oxygen partial pressure constant at 3.1 kPa. Methane oxidation rate as a function of methane partial pressure is presented in Figure 14. Reaction order for CH_4 was calculated to be 0.61.

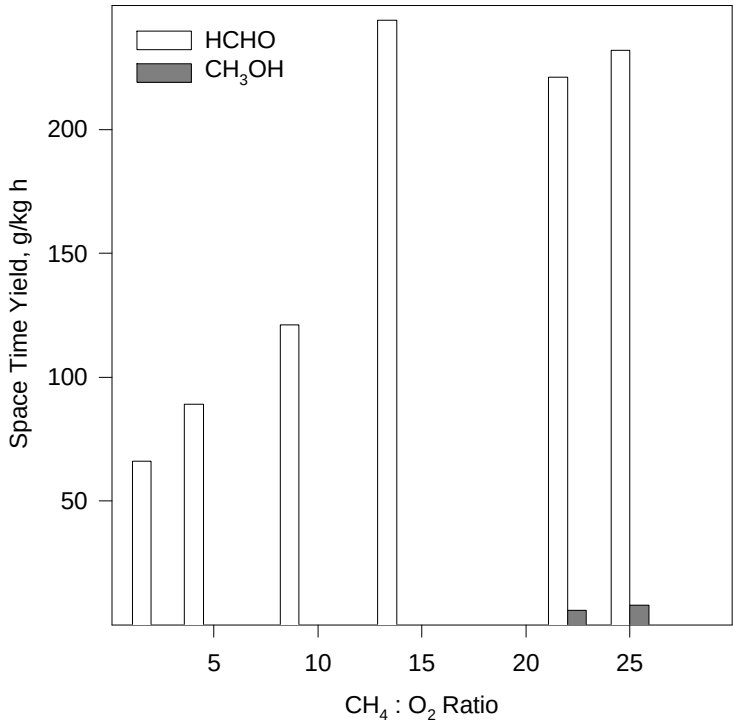

Figure 13. Space time yields of HCHO and CH_3OH over the $FePO_4(Q)/SiO_2$ as a function of CH_4:O_2 ratio. *GHSV = 12,750 hr^{-1}, T= 858 K*

Similar set of experiments were repeated at a higher oxygen partial pressure (50 kPa) and in the temperature range of 550-650^oC, and the reaction order was found to be unaffected from CH_4:O_2 ratio and temperature, in the range studied.

To determine the reaction order of oxygen for a power law rate model, oxygen partial pressure was changed in the range of 6.2 to 50.0 kPa, while keeping the methane partial pressure constant at 3.5 kPa. Results of these experiments are presented in Figure 15. Reaction order for oxygen was found to be 0.28. Experiments were repeated in the temperature range of 550-650^oC range, to observe the dependence of reaction order on temperature and no such dependence have been observed, in the temperature range studied.

Effect of steam in the feed stream was also investigated. Steam partial pressure in the feed was varied in the range of 3.1 to 9.0 kPa, which will allow to determine effect of steam partial pressure on the reaction rate. A more detailed rate model involving the steam partial pressure will be developed for the $FePO_4(Q)/SiO_2$ catalyst.

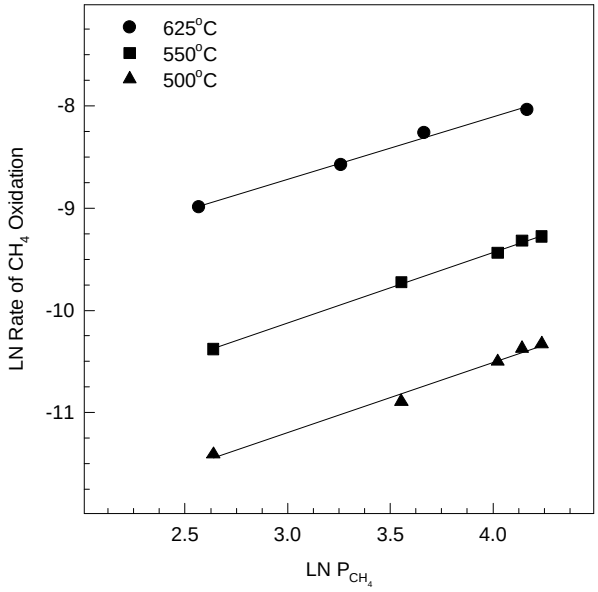

Figure.14 Effect of CH_4 partial pressure on CH_4 oxidation rate over $FePO_4(Q)/SiO_2$ catalyst. P_{CH4} *= 16.7-82.2 kPa,* P_{O2} *= 3.1 kPa, GHSV = 12,750* hr^{-1}.

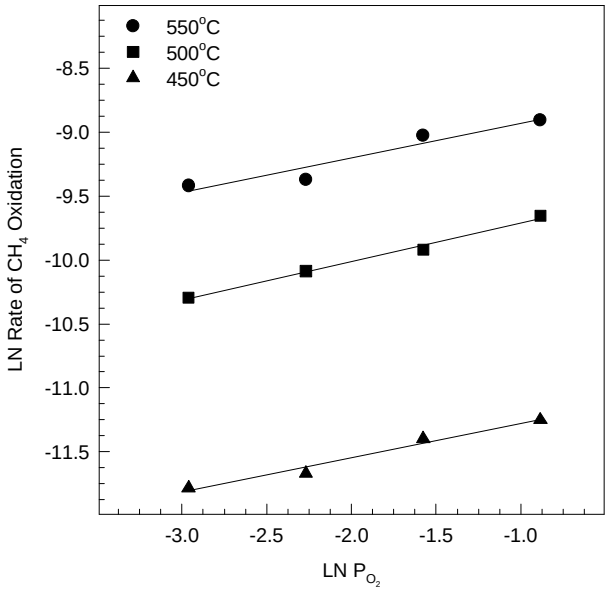

Figure.15 Effect of O_2 partial pressure on CH_4 oxidation rate over $FePO_4(Q)/SiO_2$ catalyst. P_{CH4} *= 49.8 kPa,* P_{O2} *=6.2-49.8 kPa, GHSV = 12,750* hr^{-1}.

3.1.4. $Fe_4(P_2O_7)_3$

$Fe_4(P_2O_7)_3$ was studied as a partial methane oxidation catalyst. This phase is particularly important in the preparation of more complex Fe-P-O phases. It is the precursor of β-$Fe_3(P_2O_7)_2$, which can be prepared by the solid state reaction of $Fe_2P_2O_7$ and $Fe_4(P_2O_7)_3$ at 1173 K, under vacuum. The precursor for this Fe-P-O phase was $Fe_4O_{21}P_6$•aq (~20%), which can be prepared by heating ferric nitrate and diammonium hydrogen phosphate up to 1123 K (Bonnet, et al., 1996). Precursor was activated in an air stream for 24 h, at 773 K. Activation above this temperature caused significant visual structural transformations. XRD patterns presented in Figure 16 indicates an amorphous structure both for the precursor and activated catalyst.

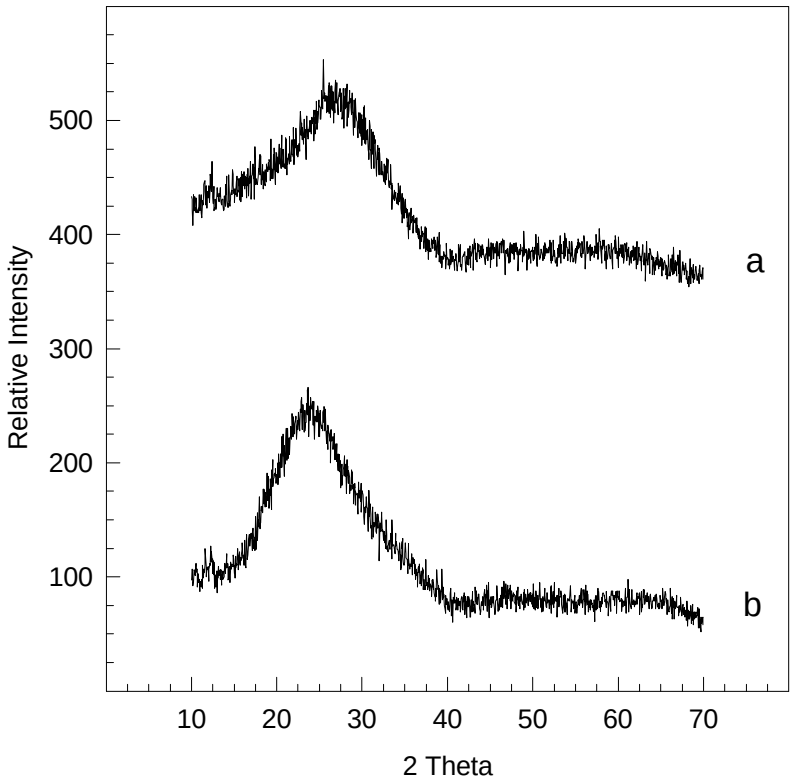

Figure 16. XRD pattern of $Fe_4(P_2O_7)_3$ **(a)** precursor, **(b)** 24 h. activated catalyst at 773 K.

When compared to $FePO_4$(Q), this catalyst was found to be less active and less selective for methane oxidation. Even formaldehyde was observed as a selective product, its space time yield was never significant (0.26-4.92 g/kg h). As the conversion-selectivity diagram given in Figure 17 indicates, CO_2 was the principal product in these experiments. This type of selectivity pattern can be explained by a direct oxidation route from CH_4 to CO_2.

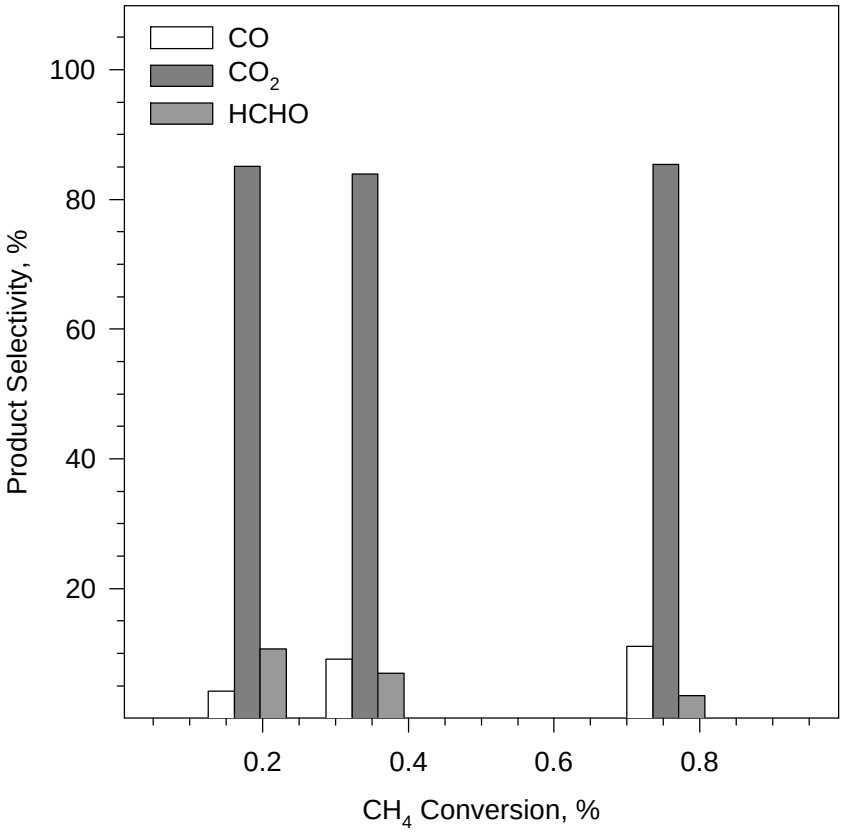

Figure 17. Product selectivity as a function of CH_4 conversion over $Fe_4(P_2O_7)_3$. *P_{CH4} = 37.6 kPa, P_{O2} = 3.1 kPa, CH_4:O_2 = 12 ,GHSV = 9,800 hr^{-1}*

Activation energy for methane oxidation was calculated as 149 kJ/mole, when a reaction order of one and zero was assumed for methane and oxygen, respectively. The exact reaction orders of CH_4 and O_2 will soon be calculated by fitting the data in a power law rate model.

The kinetic parameters calculated for the SiO_2 and Fe-P-O catalysts was listed in Table 1. Until now, $FePO_4(Q)/SiO_2$ is the only catalyst that we observed any formation of methanol when CH_4 is oxidized.

Table 1 Kinetic Parameters of CH_4 Oxidation over Fe-P-O and SiO_2 catalysts.

Catalyst	Reaction Order		Act. Energy	Reaction Rate @ 873K	STY HCHO	STY CH_3OH
	CH_4	O_2	(kj/mole)	(mol/min g)	(g/kg h)	(g/kg h)
SiO_2-OR	0.93	0.31	148	$4.8\ 10^{-5}$	96	0
SiO_2-AW	0.91	0.32	182	$5.5\ 10^{-5}$	113	0
$Fe_4(P_2O_7)_3$	NA		149	$3.7\ 10^{-6}$	4.9	0
$FePO_4$(Q)	0.66	0.45	NA	$1.7\ 10^{-5}$	59	0
$FePO_4$(Q)/SiO_2	0.61	0.28	NA	$9.9\ 10^{-5}$	487	7.9

(*) Reaction rate at 773 K.

3.2. Characterization of Fe-P-O and SiO_2 Catalysts

3.2.1. BET Surface Area Measurement

Results of BET surface area measurements of the several SiO_2 and Fe-P-O are listed in Table 2.

Table 2 BET Surface Area Measurement of Fe-P-O and SiO_2 Catalysts.

Catalysts	Surface Area (m^2/g)
$FePO_4$(Q)	8.6±0.2
$Fe_4(P_2O_7)_3$	9.1±0.2
$FePO_4$(Q)/SiO_2 (5%)	80.8±1.8
SiO_2-OR	140.4±3.1
SiO_2-NAW	621±13
SiO_2-AW	588±13

Surface area of the $FePO_4$ catalyst reported in the literature ranges form 1.8 to 15 m^2/g (Bonnet, et al., 1996 and Ai, et al., 1993), which is consistent with our results. Different precipitated silicon oxides yielded significant differences in the surface area. We can speculate that the SiO_2-AW contains micropores which is leading to a four-fold increase in the surface area. A 40 m^2/g decrease in the surface area indicates that acid washing promotes the collapse of some of these pores.

Silica supported $FePO_4$(Q) catalyst has a significantly lower surface area than the support itself (SiO_2-OR). Such a decrease in the surface area can be explained by pore blocking caused by $FePO_4$(Q) clusters. The loading level for this catalyst was 5% wt. Lower loading levels of $FePO_4$(Q) may prevent excessive pore blocking and result in a more active catalyst.

3.2.2. X-Ray Diffraction (XRD)

In our previous experiments, we observed peak sharpening and an increase in the intensity for the aged $FePO_4$(Q) when compared to the fresh catalyst. With the silica supported $FePO_4$(Q) such a trend was also evident. Peaks at 19.8 and 25.7^o were sharper and relatively intense for the 30 h. aged catalysts. These changes may be induced by further oxidation of the catalyst in the reaction conditions. To investigate this, $FePO_4$(Q) catalysts were activated longer in a furnace before the steady state experiments. 24 h and 72 h air activated catalysts revealed no difference in the X-ray diffraction patterns. These patterns are presented in Figure 18. For the determination of the kinetic parameters equilibrated catalysts were used. Peak assignment to these patterns insures that the starting catalysts used in these experiments contains only the quartz phase.

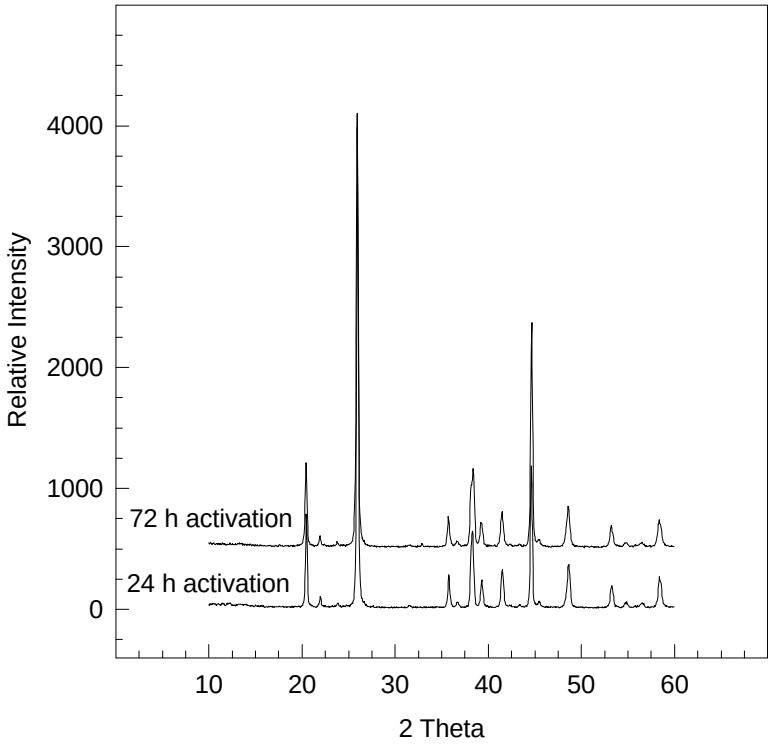

Figure 18. X-ray diffraction pattern for a 24 h and a 72 h air activated $FePO_4$(Q) catalyst.

3.2.3. FTIR

Transmission FTIR spectra of the $FePO_4$(Q) and $Fe_4(P_2O_7)_3$ catalysts are given in Figure 19 and Figure 20, respectively. In these experiments, instead of using the fast, liquid nitrogen cooled MCT detector, a TGA detector was used to acquire a wider transmittance spectrum. Most of the infrared bands corresponding the metal-oxygen and

metal-phosphorous bond vibrations and stretches are under 800 cm^{-1}. The bands observed for $Fe_4(P_2O_7)_3$ is relatively broader than $FePO_4$(Q). This information will be useful in the characterization of more complex Fe-P-O phases. The French catalyst research groups testing Fe-P-O phases as oxidative dehydrogenation catalysts for isobutaraldehyde synthesis acquired very little or no FTIR data as part of their catalyst characterization. Even there is not much literature on IR applications over Fe-P-O systems, in the next quarter a detailed literature survey will be carried on the applications of this technique to the iron phosphate catalysts.

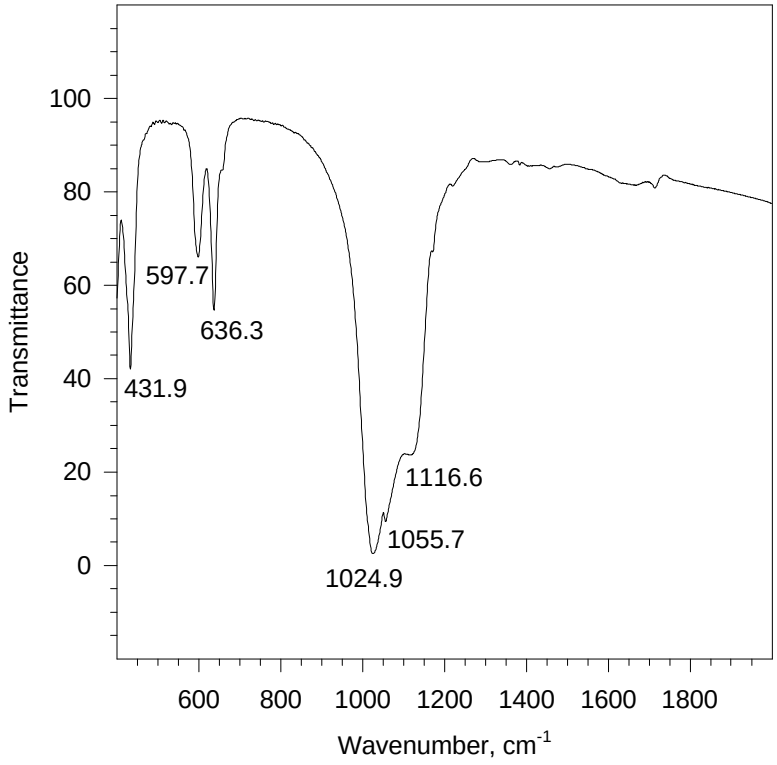

Figure 19. Transmittance spectra of $FePO_4$(Q).

Transmittance spectra of Fe_2O_3 was also acquired to make peak assignment easier. This spectrum is presented in Figure 19. The bands observed for $FePO_4$(Q) and $Fe_4(P_2O_7)_3$ have significant shifts in the frequencies in the vibrations of Fe-O bonds in 1020 cm^{-1} range. Peak assignments for these spectra will be done in the next quarter.

In situ IR experiments will be designed to investigate the changes in the catalytic chemistry and structure when water is fed.

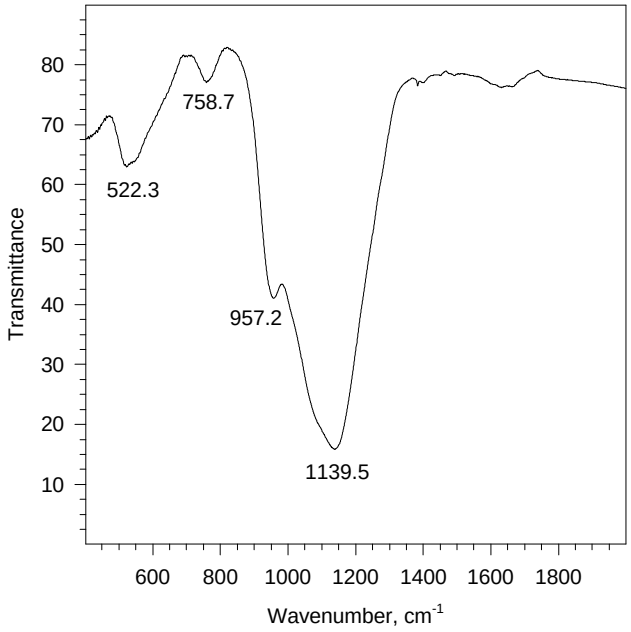

Figure 20. Transmittance spectra of $Fe_4(P_2O_7)_3$.

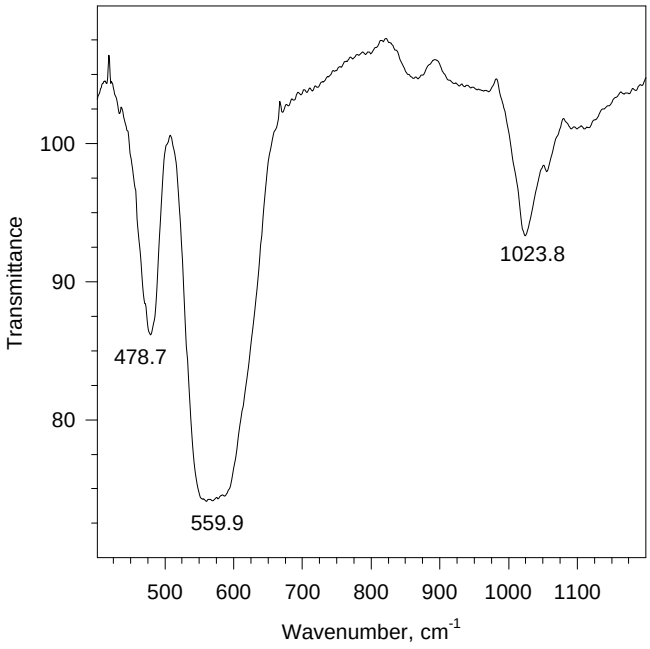

Figure 21. Transmittance spectra of Fe_2O_3.

3.2.4. Mössbauer Spectroscopy

Mössbauer spectroscopy is a very powerful technique to probe the strength of bonding of a Mössbauer atom, which will give both qualitative and quantitative information on the oxidation state, covalency, coordination number and chemical environment. There is extensive literature on the application of this technique to characterize iron phosphates.

Mössbauer spectra of various Fe-P-O catalysts were presented in Figure 22. The first catalyst presented (prep#1) is the Fe promoted vanadyl pyrophosphate (Fe-VPO). To our knowledge there is very little or no literature on the use of Mössbauer spectroscopy for Fe-promoted VPO catalysts. Even the Fe content was around 2%, the Mössbauer spectrum was successfully acquired. Second spectrum (prep #2) belongs to a new preparation, the tridymite phase of $FePO_4$, with an P:Fe ratio of 2.33. 8% wt. Cs was used in the preparation to promote the formation of the tridymite phase. Third and fourth spectra belongs to the $FePO_4(Q)/SiO_2$ and $FePO_4(Q)$ catalysts, respectively. Different shapes and positions of the peaks in these spectra indicate different Fe environments for these preparations..

Table 3 Hyperfine Interaction Parameters of Various Fe-P-O Catalysts

Catalyst	Susceptible Component	δ (mm/s)	Δ (mm/s)	Γ (mm/s)	F (%)
Fe-VPO	1	0.395 (5)	0.63 (1)	0.38 (2)	56
	2	0.393 (6)	1.10 (2)	0.38 (2)	40
	3	0.940 (6)	2.50 (2)	0.50 (1)	4
Cs-$FePO_4$ (P:Fe=2.33)	1	0.447 (3)	0.39 (1)	0.35 (1)	68
	2	0.424 (5)	0.85 (2)	0.40 (1)	32
$FePO_4(Q)/SiO_2$	1	0.380 (4)	0.61 (2)	0.38 (1)	47
	2	0.372 (4)	0.06 (3)	0.46 (1)	53
$FePO_4$ (Q)	1	0.282 (5)	0.62 (1)	0.29 (1)	93
	2	0.300 (1)	0.90 (1)	0.30 (1)	7

The hyperfine interaction parameters as δ (Isomer shift relative to α-Fe in mm/s), Δ (Quadrupole splitting in mm/s) and Γ (Full-width-at-half-maximum in mm/s) are given in Table 3. Deconvolution of the peaks indicates presence of more than one susceptible component in these samples. Fractional resonance area (F) is for these components is tabulated in the last column of Table 3. The numbers in parenthesis indicates the variation in the last digit.

The reported Mössbauer spectra were acquired very recently. A detailed literature survey is necessary for peak assignments which will be completed in the next quarter.

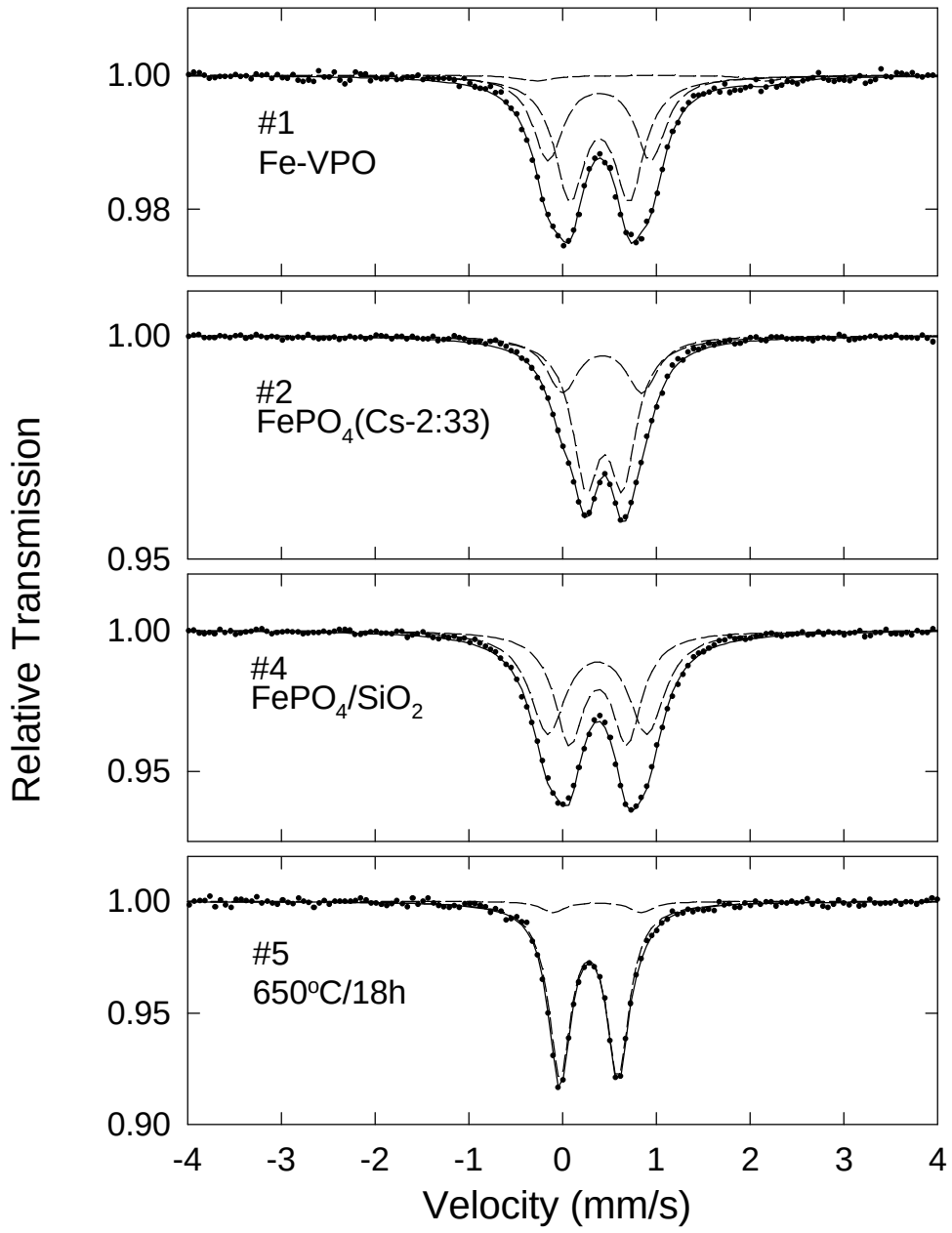

Figure 22. Mössbauer spectra of various Fe-P-O catalysts.

4. PLANNED ACTIVITIES

4.1. Reactor Studies of Fe-P-O Catalysts

In the next quarter, the following catalyst will be prepared and tested for CH_4 oxidation.

i. P_2O_5/SiO_2	1%, 2%, 5% (loading)	
ii. Fe_2O_3/SiO_2	1%, 2%, 5% (loading)	
iii. $FePO_4/SiO_2$	0.5%, %, 2%(loading)	
iv. $FePO_4$-tridymite		
with Cesium	Fe/P/Cs =	1/1.33/0.13, 1/2.66/0.13, 1/1.33/0.25, 1/2.66/0.25
without Cesium	Fe/P =	1/1.33, 1/2.66

Through these experiments the effect of catalyst loading for the supported catalysts, the effect of P:Fe ratio and the roles of iron and phosphorous in these catalysts will be investigated. These new preparations will also be characterized in detail by several surface (XPS) and bulk analysis (XRD, ICP-AA, Mössbauer spectroscopy and FTIR) techniques.

Addition of steam caused significant changes in the selectivity-conversion pattern and an increase in the space time yield of formaldehyde for the $FePO_4$(Q) and $FePO_4$(Q)/SiO_2 catalysts. Effect of steam addition will be studied, and a detailed rate model, involving steam partial pressure, will be proposed to describe the kinetics of CH_4 oxidation over these catalysts.

As a part of our advanced catalysts studies, $Fe_2(PO_3OH)P_2O_7$ the active phase for oxidative dehydrogenation reactions of saturated acids, will be examined for methane oxidation.

4.2. Publication of Results

Preparation of manuscripts for publication continues. A paper describing methane oxidation over unpromoted and transition metal promoted vanadyl pyrophosphate was submitted to *Journal of Catalysis* previously. This article is accepted for publication. Other articles currently in preparation are:

- Detailed study of kinetics of methane, methanol, formaldehyde, dimethyl ether, and perhaps CO conversion over vanadyl pyrophosphate. A draft of this paper is currently being updated and should be submitted during this quarter.
- A paper describing our methods for modification of the surface acidity of vanadyl pyrophosphate is being prepared. Some additional data may be required before publication.
- A note on CH_4 partial oxidation over iron phosphates will be prepared and submitted during the next quarter.

- A presentation describing most of the aspects of this project will be given at the American Institute of Chemical Engineers Meeting AIChE-97, "Fundamentals of Oxide Catalysis" section, in Los Angeles during November.

5. REFERENCES

Ai, M. J. Catal. 101 389 (1986).

Ai, M., Muneyama, E., Kunishige, A., Ohdan, K., J. Catal. 144 632 (1993).

Bonnet, P., Millet, J.M.M., J. Catal. 161 198 (1996).

Busca, G., Centi, G., Trifiro, F., Lorenzelli, V. J. Phys. Chem. 90 1337 (1986a).

Busca, G., Cavani, F., Centi, G., Trifiro, F. J. Catal. 99 400 (1986b).

Busca, G., Centi, G. J. Am. Chem. Soc. 111 46 (1989).

Centi, G., Trifiro, F., Ebner, J.R., Franchetti, V.M. Chem. Rev. 88 55 (1988).

Cornaglia, L.M., Lombardo, E.A. Appl. Catal. A General 127 125 (1995).

Horowitz, H.S., Blackstone, C.M., Sleight, A.W., Teufer, G. Appl. Catal. 38 193 (1988).

Hutchings, G.J. Appl. Catal. 72 1 (1991).

Kastanas, G.N., Tsigdinos, G.A., Schwank, J., J. ACS Div. Petr. Chem. Prepr. 33 3 393 (1988).

Michalakos, P.M., Kung, M.C., Jahan, I., Kung, H.H. J. Catal. 140 226 (1993).

Millet, J.-M. M., Vedrine, J.C. Appl. Catal. 76 209 (1991).

Muneyama, E., Kunishige, A., Ohdan, K., Ai, M. J. Catal. 158 378 (1996).

Parmaliana, A., Frusteri, F., Miceli, D., Mezzapica, A., Scurell, M.S., Giordiano, N., Appl. Catal. 78 7 (1991).

Spencer, N.D., Pereira, C.J. J. Catal. 116 399 (1989).

Wang, Y., Otsuka, K. J. Catal. 155 256 (1995).